Proc. Natl. Acad. Sci. USA
Vol. 92, pp. 569–573, January 1995
Biophysics

Nanosecond time-resolved circular polarization of fluorescence: Study of NADH bound to horse liver alcohol dehydrogenase

(optical activity/circularly polarized luminescence/excited-state dynamics/fluorescence lifetime)

JOSEPH A. SCHAUERTE*†, BRUCE D. SCHLYER*, DUNCAN G. STEEL*‡, AND ARI GAFNI*†§

*Institute of Gerontology and Departments of †Biological Chemistry and of ‡Physics and Electrical Engineering, University of Michigan, Ann Arbor, MI 48109

Communicated by J. L. Oncley, University of Michigan, Ann Arbor, MI, October 7, 1994 (received for review January 3, 1994)

ABSTRACT **Circularly polarized luminescence (CPL) spectroscopy provides information on the excited-state chirality of a lumiphore analogous but complementary to information regarding the ground-state chirality derived from circular dichroism. The sensitivity of CPL spectra to molecular conformation makes this technique uniquely suited for the study of biomolecular structure, as extensively demonstrated in earlier studies. Unfortunately, the CPL spectra of many biomolecules often contain significantly overlapping contributions from emitting species either because multiple lumiphores are present (e.g., tryptophan residues in a protein) or because multiple conformations of the biomolecule simultaneously exist, each with a unique CPL spectrum. Increased resolution between individual contributions to the CPL may be achieved by time-resolving this signal, thus taking advantage of the fact that, as a rule, each of the emitting species also has a characteristic decay time associated with its electronically excited state. In addition, the time resolution provides information regarding dynamics associated with the different chiral states of the system. The present study describes an instrument for the determination of time-resolved CPL (TR-CPL) with subnanosecond resolution and its application to several chiral systems. The technique was first demonstrated on a model system with a strong time-dependent CPL signal. Subsequently, the circularly polarized component in the fluorescence of reduced nicotinamide adenine dinucleotide (NADH) bound to liver alcohol dehydrogenase was time-resolved. The CPL of NADH in the binary enzyme–coenzyme complex is time-dependent, reflecting structural differences around the reduced nicotinamide possibly due to a dynamic restructuring. In contrast, the CPL of the coenzyme in the ternary complex formed with enzyme and the substrate analog isobutyramide is essentially time-independent, likely reflecting a more rigid binding domain. Since the linear polarization of the fluorescence of the two complexes did not show any local flexibility of the NADH chromophore, the excited-state conformational rearrangement of the binary complex indicates a subtle change in its interactions with group(s) in direct contact with it.**

Circular dichroism (CD) and circular polarization of luminescence (CPL) arise from the chirality of the ground state and of the excited state of the observed chromophore, respectively, and have found extensive use in structural studies of biomolecular systems (1–3). These two optical activity techniques utilize the differential interactions of chiral chromophores with left and right circularly polarized light as expressed by the unitless anisotropy factors for absorption (g_{ab}) and emission (g_{em}):

$$g_{ab} = \frac{\Delta\varepsilon}{\varepsilon} = \frac{\varepsilon_l - \varepsilon_r}{\varepsilon} = \frac{4\nu}{\nu_{kj}} \frac{R_{kj}}{|\langle j|\boldsymbol{\mu}|k\rangle|^2}$$

and

$$g_{em} = \frac{\Delta I}{I/2} = \frac{4\nu}{\nu_{jk}} \frac{R_{jk}}{|\langle k|\boldsymbol{\mu}|j\rangle|^2}, \quad [1]$$

where ε = molar absorptivity, ε_l and ε_r = left and right molar absorptivity, I = intensity, ν = frequency, $R_{kj} = \mathrm{Im}\{\langle j|\boldsymbol{\mu}|k\rangle\langle k|\mathbf{m}|j\rangle\}$, $\boldsymbol{\mu} = e\Sigma_i \mathbf{r}_i$, $\mathbf{m} = e/2mc\Sigma_i \mathbf{r}_i \times \mathbf{p}_i$, and the sum is over all electronic states.

While CPL spectra are sensitive to the structure surrounding the lumiphore, their applicability to studies of complex biomolecules is limited by the fact that as a rule these molecules contain several identical lumiphores in different environments (e.g., tryptophan residues in a protein). Moreover, the ensemble of biomolecules in solution frequently exists in an equilibrium among different conformational states that interconvert on a time scale longer than that involved in the emission of luminescence. Hence, a typical CPL spectrum is a superposition of several independent contributions with a high degree of spectral overlap. One effective approach for the resolution of such composite spectra is by monitoring the time evolution of the CPL signal and the luminescence decay after electronic excitation of the lumiphore and correlating the CPL components to those obtained from analysis of the luminescence decay. Individual terms in the CPL may then be assigned distinct decay components. Time-dependent CPL may also arise from excited-state interactions of the lumiphore that affect the local chiral properties during the excited state lifetime. In such cases each lumiphore may possess a time-dependent CPL, and the time-resolved CPL (TR-CPL) then can be used to obtain information on the dynamics of excited-state interactions.

We have recently utilized time-resolved optical activity and demonstrated that we could assign each of the four components obtained in the analysis of the decay of the room-temperature phosphorescence of bacterial glucose-6-phosphate dehydrogenase (G6PDH) with a time-independent g_{em} derived from the analysis of the time-resolved circularly polarized phosphorescence from the enzyme's tryptophan residues (4). This assignment allowed us to conclude that the room-temperature phosphorescence of G6PDH originates in three or four tryptophan residues, each with a unique, time-independent CPL contribution.

In the present work we discuss the design and application of a new TR-CPL spectrometer that enables the determination of $g_{em}(t)$ values as small as 10^{-4} with subnanosecond resolution, thus enabling us to follow changes in the CPL on the short-time scale (nsec) typical of protein fluorescence decay. This capability was demonstrated on a model system by recording the

The publication costs of this article were defrayed in part by page charge payment. This article must therefore be hereby marked "*advertisement*" in accordance with 18 U.S.C. §1734 solely to indicate this fact.

Abbreviations: CPL, circularly polarized luminescence; TR-CPL, time-resolved CPL; IBA, substrate analog isobutyramide; LADH, horse liver alcohol dehydrogenase; PHA, pulse-height analysis; TAC, time-to-amplitude converter; TDC, time-to-digital converter; TCSPC, time-correlated single-photon counting; CAMAC, computer interface standard.

§To whom reprint requests should be addressed

TR-CPL signal generated by (+)- and (−)-camphorquinone placed in the two compartments of a tandem cuvette, with the fluorescence decay time of one enantiomer being shortened by quenching to create the time-dependent optical activity. In subsequent experiments we have time-resolved the circularly polarized emission of reduced nicotinamide adenine dinucleotide (NADH) bound to horse liver alcohol dehydrogenas (LADH) in the binary complex as well as in the tight ternary complex formed in the presence of the substrate analog isobutyramide (IBA). The steady-state CPL spectra of these two complexes have been previously reported to differ, reflecting the different microenvironments of the reduced nicotinamide ring (5). The TR-CPL results extend this knowledge. The binary complex shows a time-dependent CPL, while the optical activity of the ternary complex is essentially time-independent. These results are interpreted in the context of a model that incorporates earlier observations based on steady-state CPL and CD and provides new insight into the origin of the nonexponential decay of NADH in the ternary complex with LADH and IBA.

Time-resolved emission portrays a more refined picture of the system being studied by allowing the assignment of unique spectral properties to individual decay components. This has been utilized to resolve the steady-state fluorescence spectra of complex systems into their decay-associated spectra (6). We now demonstrate that TR-CPL can be used in an analogous way to obtain additional information pertaining to excited state chirality, thereby enabling more detailed structural analysis.

MATERIALS AND METHODS

LADH was purchased from Boehringer Mannheim. NADH, camphorquinone, and other reagents were purchased from Sigma and used without further purification. Before being used for experiments, LADH was dialyzed for 8 hr against three changes of 100 mM phosphate buffer (pH 7.4), and precipitated protein was filtered through 0.2-μm filters (Gelman). Enzyme assays were done according to established procedures (7). In all experiments enzyme activities were within a few percent of published values. CD studies were performed on a Jasco (Easton, MD) model J-720 spectropolarimeter using a 1-cm-path-length quartz cuvette and 1-nm bands.

The design of the instrumentation used in the present study followed the conceptual approach reported earlier for measuring time-resolved circularly polarized emission on the microsecond-to-second time scale (4). To obtain subnanosecond time resolution with adequate dynamic range and linearity, the present approach uses time-correlated single-photon counting (TCSPC). Use of the conventional method of TCSPC based on analog time-to-amplitude converters (TAC) and pulse-height analysis (PHA) was not viable because of the limited data acquisition rate in this approach. More specifically, we note that detection of CPL over a given time interval (typically a fraction of a fluorescence lifetime) at the level of 1 part in 10^4 requires collection of $>10^8$ photons over that interval (assuming Poisson statistics). Using the TAC–PHA approach requires many hours to obtain adequate time resolution over several fluorescence lifetimes, limiting the usefulness of such a procedure. To overcome this problem so as to obtain over an order-of-magnitude increase in the data collection rate, we used a high-speed time-to-digital converter (TDC) and histogramming memory [computer interface standard (CAMAC; Institute of Electrical and Electronic Engineers, 583/596)-based electronics]. Indeed, even faster data collection rates are possible by establishing multiple-channel TDCs, a feature critical for use of this system in real-time studies of protein folding and dynamics.

A schematic representation of the instrumentation developed to measure TR-CPL is provided in Fig. 1. A Hinds Instruments (Hillsboro, OR) model PEM-90 photoelastic modulator operating at 42 kHz, aligned with a UV-transmissive linear polarizer [Oriel (Stamford, CT) model 27320], modulates left- and right-handed circular polarization emitted by the sample. The sample emission is detected by TCSPC apparatus based on a LeCroy (Chestnut Ridge, NY) model 4204 TDC. The TDC is gated by a Stanford Research (Sunnyvale, CA) delay gate generator (model 535), which is driven by the reference output of the photoelastic modulator. The gates defined by the delay gate generator correspond to maximum transmission of right and left circularly polarized light during the photoelastic modulation cycle. Differences in intensity of emission collected during these gates correspond to nonzero chiral emission from the sample (4).

The LeCroy TDC used here operates within a LeCroy 8025 CAMAC crate that is interfaced to a computer (Apple Macintosh Quadra 700) through a Kinetic Systems (Spring Valley, NY) model 3922 crate controller and 2932 Nubus interface. The CAMAC instrumentation was controlled by the Macintosh through KMAX software (Sparrow, Mississippi State, MS). Data generated in the TDC is stored in a LeCroy model 3588 histogramming memory. Pulses from the sample [start pulse detected by a Hamamatsu (Middlesex, NJ) model 1527 photomultiplier tube and the stop pulse detected by a Hamamatsu model R928 photomultiplier tube] are routed through a CAMAC constant fraction discriminator [Ortec (Oak Ridge, TN) model CCF8200]. Data throughput is up to 800 kHz

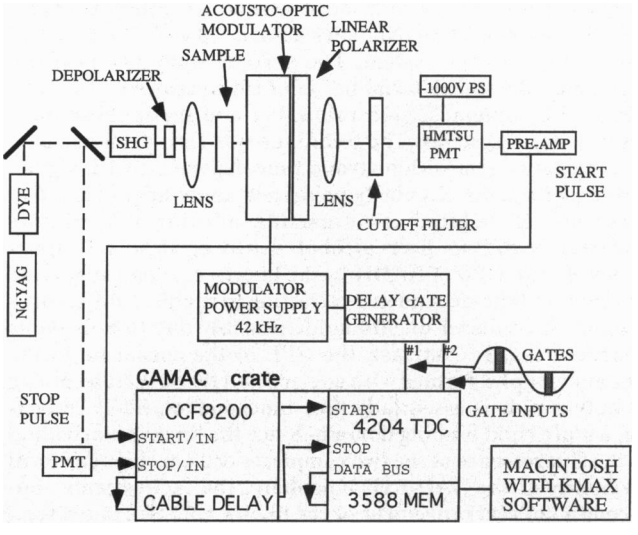

FIG. 1. Block diagram of the TR-CPL instrument. The instrument is based on the time-correlated single-photon counting technique used in reverse mode. However, the use of a TAC with subsequent PHA is replaced with a single component, a TDC, which directly measures time between start and stop signals and, within a microsecond, stores the information via a "fast bus" in the histogramming memory (MEM) module. The fluorescence decay is measured by correlating the time between the excitation pulse and the emission of fluorescence by the sample over a large number of decay events. Two windows are established within the histogramming memory, and the decay data are sent to one or the other depending upon the timing of gates established by the photoelastic modulator and delay gate generator. Left and right circularly polarized signals are thus simultaneously recorded. To minimize the pulse pileup distortion of the data, counts are collected at a rate $< 2\%$ of the cavity-dumping frequency of the dye laser (i.e., of stop pulses). In the reverse-counting mode, the sample emission triggers the start pulse of the TDC, while the stop pulse is the excitation source delayed by coaxial cable. SHG, second harmonic generation; HMTSU, Hamamatsu; PS, power supply; PMT, photomultiplier tube; Nd:YAG, neodymium/yttrium/aluminum garnet laser.

between the TDC and the histogramming memory. The dwell period of the TDC was set to 156 psec. It should be noted that pulse pileup artifact is reduced by collecting <2% of the excitations (8). The cavity-dumping rate was 10 MHz compared with 1 MHz used with the TAC–PHA system, increasing the collection rate 10-fold compared with the previous TCSPC collection rate of 20 kHz (9) determined by the analog-to-digital conversion rate of the pulse-height analyzer and reset time of the TAC (9). It should be noted that the current system actually allows for even higher repetition rates (up to 40 MHz). Results of the fluorescence-decay analysis were comparable to those obtained by high-resolution time-resolved fluorescence-decay measurements (dwell times < 50 psec per channel) of the NADH–LADH complex in binary and ternary complexes as measured by TAC-PHA-based instrumentation described elsewhere (10).

Excitation of samples was done by a frequency-doubled [INRAD (Northvale, NJ) SHG], synchronously pumped cavity-dumped mode-locked dye laser [Coherent Radiation (Palo Alto, CA) model 701-3] pumped by a continuous-wave mode-locked YAG (yttrium/aluminum garnet) laser [Quantronix (Smithtown, NY) model 416 or Coherent Antares]. The excitation wavelength was either 300 or 308 nm, and the emission band was selected by a KV418 (Schott, Duryea, PA) high-pass cutoff filter. Calibration of the instrument was done by introducing known amounts of circular polarization into the luminescence of fluorescein (depolarized with Oriel model 28115) as described before (11).

The fluorescence decay and TR-CPL were analyzed by a Marquadt (12) nonlinear least-squares procedure that assumed photon-counting statistics [Photon Technology International (South Brunswick, NJ) FLDEC, MEM, and ESM programs]. Since the standard deviation for g_{em} in a given data channel varies as $\sqrt{(2/n)}$ (n is the number of counts in that channel), the noise in TR-CPL plots tends to increase across the luminescence intensity decay. To compensate for this effect and to achieve a representation where the error bars for each data point (at longer times) were approximately the same, we successively grouped together adjacent channels to achieve an approximately equal number of counts for each of the data points presented in Figs. 2 and 3.

To generate a known TR-CPL signal, solutions of (+)- and (−)-camphorquinone in chloroform were placed in the two halves of a tandem cuvette, and the emission of one of the antipodes was dynamically quenched by the addition of iodomethane so as to generate a biexponential decay. Data used to generate the TR-CPL spectrum included about 300 million counts.

The TR-CPL data for the binary and ternary complexes of LADH–NADH included ≈900 million total counts for the left and right circular polarization channels for the binary complex and 500 million for the ternary complex. Several experiments

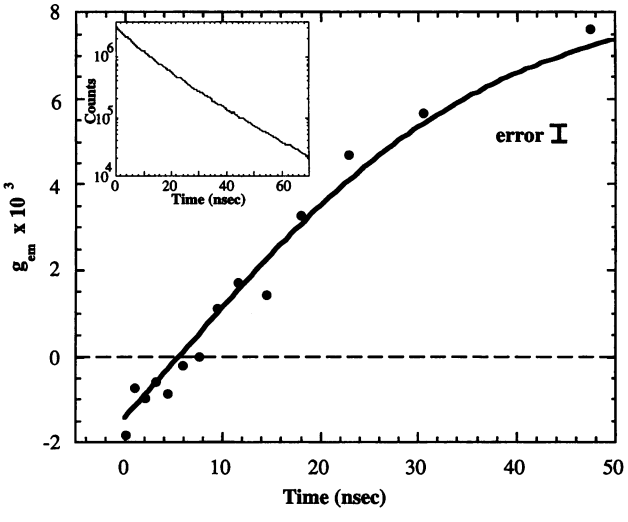

FIG. 2. Time-resolved anisotropy factor for the combined emission from (+)- and (−)-camphorquinone solutions in chloroform (6 mM and 12 mM, respectively) placed in the two compartments of a tandem cuvette. Emission was excited at 300 nm and observed through a KV418 filter. The decay kinetics of each antipode is monoexponential with a lifetime of 16.3 nsec. To generate time dependency in g_{em}, the emission of (−)-camphorquinone was dynamically quenched by 100 mM iodomethane to give a lifetime of 7.5 nsec. (*Inset*) Decay kinetics of the combined emission, which was biexponential as expected, with lifetimes of 16.3 and 7.5 nsec, and preexponential factors of 0.4 and 0.6, (assigned to the (+) and (−) antipodes respectively). Each enantiomer of camphorquinone was found to display a time-independent CPL with equal and opposite g_{em} values ($\pm 8.4 \times 10^{-3}$). The g_{em} values presented were obtained by using the approach described in *Materials and Methods*, by adding the single-photon counts in adjacent data channels to yield about 16×10^6 counts, giving a (constant) standard deviation for g_{em} of 3.5×10^{-4}. The solid line is the theoretical fit to the data generated by using Eq. **2** and the values for the decay times in nanoseconds and preexponentials listed above.

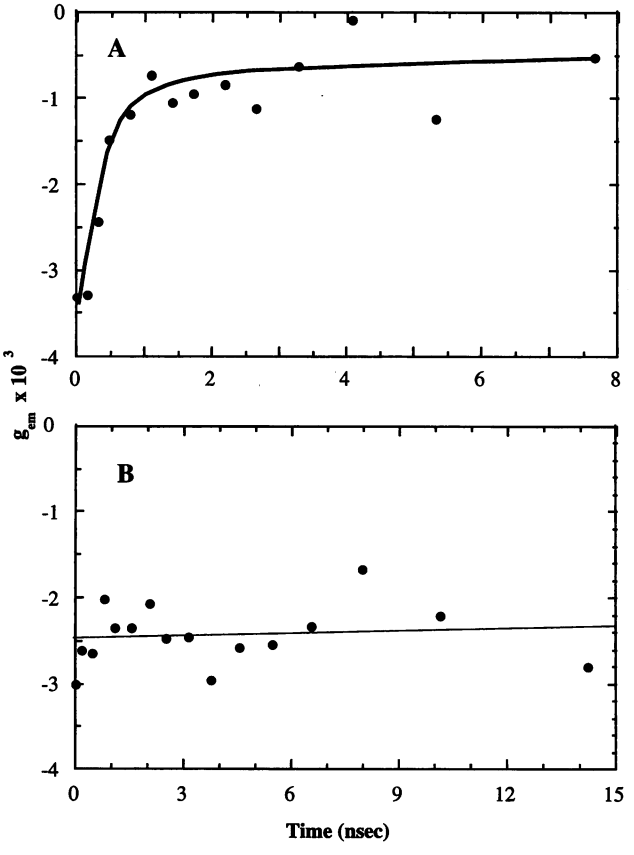

FIG. 3. Time-resolved circularly polarized fluorescence of NADH bound to LADH in binary (*A*) and ternary (*B*) complexes. Excitation was at 308 nm to minimize tryptophan absorbance, and emission was monitored above 418 nm. The decays for right and left circularly polarized light of each experiment were independently stored in the histogramming memory after an experiment. The individual left and right fluorescence decay data from the histogramming memory windows were independently analyzed (Photon Technology International MEM software), and then the theoretical fit was recombined with the residuals to produce decay data (with original noise) deconvoluted from the instrument response function. The time dependence of $g_{em}(t)$ was then constructed by combining the left and right fluorescence decays according to Eq. **1**. The photon counts were added within the decay as described in *Materials and Methods* to give a minimum of 6×10^7 (binary complex) or 3×10^7 (ternary complex) for each gem data point. This corresponds to a standard error of 1.8×10^{-4} for the binary and 2.6×10^{-4} for the ternary complex.

were added together so that samples did not receive excessive exposure to UV irradiation.

RESULTS AND DISCUSSION

The fluorescence emitted by a lumiphore is sensitive to the surrounding microenvironment, a property that has been extensively utilized in the study of biomolecular structure, interaction, and dynamics. Additional structural information can be obtained by using the optical activity associated with the absorption or emission of the chromophore through the CD or CPL (1–3), which reflect the chirality of the chromophore in the ground or excited state, respectively. TR-CPL measurements provide additional information by enabling one to resolve contributions to the optical activity from components with different decay times, thus providing a means to differentiate between different emitters. CPL spectra associated with one lumiphore in several chiral environments, as in the case of protein conformational heterogeneity, can also be resolved. Moreover, changes in the optical activity of a lumiphore following electronic excitation (as due to realignment of the excited chromophore relative to its domain) can be followed through the time dependence of the emission anisotropy factor. Techniques based on time-resolved optical activity measurements are demonstrated by recent work in other laboratories for both absorption (13) and emission (14, 15) in the millisecond regime of chromophores in chiral environments.

The present communication describes an instrument that enables the study of TR-CPL with subnanosecond resolution and with high sensitivity, allowing the accurate recording of anisotropy factors in the range of 10^{-4}–10^{-3}, typical of biomolecular CPL. The performance of this instrument was first tested by engineering a known TR-CPL signal by using the mixed emissions of (+)- and (−)-camphorquinone as described in *Materials and Methods*. Fig. 2 presents the fit between the experimental data and the $g_{em}(t)$ curve predicted by the equation:

$$g_{em}(t) = \frac{g_+\alpha_+ e^{-t/\tau_+} + g_-\alpha_- e^{-t/\tau_-}}{\alpha_+ e^{-t/\tau_+} + \alpha_- e^{-t/\tau_-}} \quad [2]$$

where g_+ and g_- are the experimentally determined time-independent emission anisotropy factors of pure (+)- and (−)-camphorquinone, respectively; and α_+, α_-, τ_+, and τ_- are the respective preexponential factors and decay times for the two antipodes obtained from a biexponential fit to the total luminescence decay obtained in the tandem cuvette (Fig. 2 *Inset*). The excellent agreement between the experimental results and the values predicted from Eq. **2** clearly demonstrates the capability of the instrumentation to accurately determine g_{em} values with nanosecond resolution.

The time evolution of the CPL of NADH bound to LADH in the binary complex and in the ternary complex with IBA was also recorded and is presented in Fig. 3. A striking difference between these two complexes is evident: the anisotropy factor of the binary complex (Fig. 3*A*) is strongly time-dependent and decays from an initial value of -3.3×10^{-3} to a limiting value of -5×10^{-4}. In contrast, the anisotropy factor of the ternary complex (Fig. 3*B*) is nearly time independent with a value of -2.5×10^{-3} in good agreement with that found in steady-state CPL measurements (5). Time integration of the $g_{em}(t)$ of the binary complex yields a value of -1.3×10^{-3}, again close to that obtained in steady-state CPL (5).

Fig. 4 presents the CD spectra of NADH in the binary complex with LADH and in the ternary LADH–NADH–IBA complex. In contrast to the steady-state CPL signals mentioned above, the CD spectra of these two complexes are practically identical, in agreement with previous reports (5, 16), and the anisotropy factor calculated from the CD and

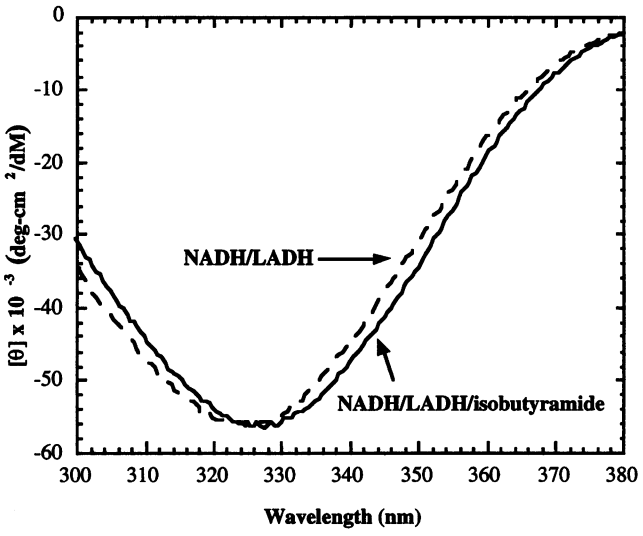

FIG. 4. CD of 140 μM NADH bound to 70 μM LADH in binary and ternary (with 100 mM isobutyramide) complexes. Data are adjusted for the presence of unbound NADH (evaluated with a K_d of 0.5 μM and 5 nM for binary and ternary complexes, respectively).

absorption spectra according to Eq. **1** is -2.8×10^{-3}, in good agreement with the value previously reported (5, 16). The identical ground-state optical activities of NADH in the binary and ternary complexes have been interpreted in earlier work to reflect identical chiral environments in the nicotinamide binding site in the two complexes.

NADH emission originates in the reduced nicotinamide ring and is greatly enhanced upon binding to LADH, with further enhancement upon formation of the ternary complex LADH–NADH–IBA (17–19). These increases are due to unstacking of the adenine and nicotinamide rings of the coenzyme and to shielding of the fluorophore from aqueous solvent as shown by crystallographic studies (20). The increased fluorescence of the ternary complex apparently reflects its higher rigidity (5, 18, 19, 21). The fluorescence of NADH, both free and LADH-bound, has previously been found to decay nonexponentially, an observation that was explained in terms of either ground-state heterogeneity (18) or excited-state interaction of the nicotinamide ring (19). Our data (not shown) confirms the nonexponentiality of the fluorescence decay of both binary and ternary complexes, which can be fit well by three and two exponentials, respectively.

The CD spectra shown in Fig. 4 reveal that the optical activities of the binary and ternary complexes in their ground state are identical. In contrast, it has been shown that the excited-state chiral environments of NADH in the binary and ternary complexes are different, as evidenced by their different steady-state CPL spectra (5). The TR-CPL of the two complexes presented in Fig. 3 clearly reveal that a significant contribution of this difference is in a dynamic evolution of the anisotropy. More specifically, while the optical activity in the excited state of the ternary complex is essentially time-independent and similar to that of the ground state, the excited state optical activity of the binary complex is strongly time dependent, and, following excitation, the system evolves to an asymptotic value. Hence, the difference in the steady-state CPL measurements reflects a dynamic drift in the effective chiral environment.

In extracting structural information from the above data, we note that the nonexponentiality of the fluorescence decay of the ternary complex has been reported before and has been attributed to either ground-state heterogeneity—a possibility suggested by the fact that LADH is known to exist in solution in equilibrium between "open" and "closed" conforma-

tions—or to the presence of a reversible excited-state reaction involving a dark (i.e., nonradiating) state. The nearly time-independent CPL of the ternary complex is compatible with the second hypothesis but imposes a further restriction on the first model, since the different conformers have the same chirality though they differ in conformation sufficiently to affect their respective lifetimes. The fluorescence decay of the binary LADH–NADH complex is considerably more nonexponential, and the anisotropy factor is time dependent. While this behavior could again be due to increased ground-state heterogeneity, we recall that the CD of both complexes are identical—i.e., no significant change occurs in the NADH-binding site when IBA is added, despite the "tightening" of the complex reflected by the large increase in coenzyme binding constant. Hence, it seems more likely that the binary complex is characterized by a more flexible binding site that undergoes a structural rearrangement around the reduced nicotinamide ring after its electronic excitation. We believe this rearrangement to be subtle and to not involve a large movement of the nicotinamide ring relative to its binding domain but rather to involve a specific change in its interactions with groups in proximity to it. This assertion is based on time-resolved linear-polarization studies of the binary complex (data not shown), which show a time-independent anisotropy reflecting no movement of the coenzyme relative to its binding site.

In summary, time-resolved spectroscopy enhances the resolution by allowing the assignment of unique decay constants to spectral components. We have recently exploited this approach to time-resolve the circularly polarized phosphorescence of several proteins in solution, which decays on the time scale of milliseconds. The present study greatly improves the time resolution to the nanosecond range, allowing time resolution of the chirality of the excited singlet state. Since fluorescence is more common than phosphorescence in biological systems, time-resolved circularly polarized fluorescence is a powerful tool for structural studies of such molecules.

This research was supported by Grant AG09761 from the National Institute on Aging and by Grant N00014-91-J-1938 from the Office of Naval Research. B.D.S. was supported in part by a training grant from the National Institute on Aging (Contract T32AG00114).

1. Riehl, J. P. & Richardson, F. S. (1986) *Chem. Rev.* **86,** 1–16.
2. Steinberg, I. Z. (1978) *Methods Enzymol.* **49,** 179–199.
3. Steinberg, I. Z. (1975) in *Concepts in Biochemical Fluorescence*, eds. Chen, R. F. & Edelhoch, H. (Dekker, New York), Vol. 1, pp. 79–112.
4. Schauerte, J. A., Steel, D. G. & Gafni, A. (1992) *Proc. Natl. Acad. Sci. USA* **89,** 10154–10158.
5. Gafni, A. (1978) *Biochemistry* **17,** 1301–1304.
6. Knutson, J. R., Walbridge, D. G. & Brand, L. (1982) *Biochemistry* **21,** 4671–4679.
7. Valle, B. L. & Hoch, F. L. (1955) *Proc. Natl. Acad. Sci. USA* **41,** 327–338.
8. Harris, C. M. & Selinger, B. K. (1979) *Aust. J. Chem.* **32,** 2111–2129.
9. O'Connor, D. V. & Phillips, D. (1984) *Time-Correlated Single Photon Counting* (Academic, London), pp. 132–157.
10. Schauerte, J. A. & Gafni, A. (1989) *Biochemistry* **28,** 3948–3954.
11. Steinberg, I. Z. & Gafni, A. (1972) *Rev. Sci. Instrument.* **43,** 409–413.
12. Marquadt, D. W. (1963) *J. Soc. Independ. Appl. Math.* **11,** 431–441.
13. Lewis, J. W., Goldbeck, R. A., Kliger, D. S., Xie, X., Dunn, R. C. & Simon, J. D. (1992) *J. Phys. Chem.* **96,** 5243–5254.
14. Metcalf, D. H., Bolander, J. P., Driver, M. S. & Richardson, F. S. (1993) *J. Phys. Chem.* **97,** 553–564.
15. Rexwinkel, R. B., Meskers, S. C. J., Riehl, J. P. & Dekkers, H. P. J. M. (1993) *J. Phys. Chem.* **97,** 3875–3884.
16. Luisi, P. L., Olomucki, A., Baici, A., Joppich-Kuhn, R. & Thome-Beau, F. (1977) in *Pyridine Nucleotide-Dependent Dehydrogenases*, ed. Sund, H. (de Gruyter, Berlin), pp. 472–482.
17. Krishnamoorthy, G., Periasamy, N. & Venkataraman, B. (1987) *Biochem. Biophys. Res. Commun.* **144,** 387–392.
18. Visser, A. J. W. G. & van Hoek, A. (1981) *Photochem. Photobiol.* **33,** 35–40.
19. Gafni, A. & Brand, L. (1976) *Biochemistry* **15,** 3165–3171.
20. Eklund, H., Samama, J.-P. & Jones, T. A. (1984) *Biochemistry* **23,** 5982–5996.
21. Theorell, H. & McKinley-McKee, J. S. (1961) *Acta Chem. Scand.* **15,** 1811–1833.